Eur. Phys. J. D **15**, 181–188 (2001)

THE EUROPEAN PHYSICAL JOURNAL D

EDP Sciences

Determination of the helium-4 mass in a Penning trap

S. Brunner, T. Engel, A. Schmitt, and G. Werth[a]

Institut für Physik, Universität Mainz, 55099 Mainz, Germany

Received 30 March 2001

Abstract. We have measured the cyclotron frequencies of He^+, H_2^+ and D_2^+ ions in a room temperature Penning trap. The resonances were detected destructively by a time-of-flight technique. The statistical uncertainty of the resonance frequencies was generally below 1 ppb. A detailed account of measures to minimize systematic frequency shift is presented. Using the accepted values for the proton and deuteron mass we obtain a value for the ^{4}He mass: $M(^4\mathrm{He}) = 4.002\,603\,248\,9\,(22)$ (0.5 ppb). It is in agreement with the accepted value.

PACS. 27.10.+h $A \leq 5$ – 32.10.Bi Atomic masses, mass spectra, abundances, and isotopes – 07.75.+h Mass spectrometers

1 Introduction

The masses of atoms and nuclei represent one of the most fundamental properties of these systems. Their measurement has been pursued since a long time with increasing precision. A significant step towards higher accuracy has been the introduction of Penning ion traps [1,2] into mass spectrometry. Charged particles are confined by static electric and magnetic fields for very long times and their cyclotron frequency $\omega_\mathrm{c} = (e/m)B$ in a strong magnetic field B is determined. The ratio of cyclotron frequencies of two different ions in the same magnetic field gives directly their mass ratio.

The properties of Penning traps have been extensively treated in the literature [1,2] . In the ideal case the electric trapping potential has a quadrupolar shape

$$\Phi = \frac{V_0}{2d^2}\left(z^2 - \frac{\rho^2}{2}\right) \tag{1}$$

where d is a characteristic dimension of the trap and V_0 the applied voltage between ring and endcap electrodes.

The motion of a single particle of charge q and mass m in such a potential is given by three harmonic oscillations of frequencies

$$\omega_z = \left[\frac{eV_0}{md^2}\right]^{1/2}, \tag{2}$$

$$\omega_\mathrm{c}' = \frac{\omega_\mathrm{c}}{2} + \left[\frac{\omega_\mathrm{c}^2}{4} - \frac{\omega_z^2}{2}\right], \tag{3}$$

$$\omega_\mathrm{m} = \frac{\omega_\mathrm{c}}{2} - \left[\frac{\omega_\mathrm{c}^2}{4} - \frac{\omega_z^2}{2}\right]^{1/2}. \tag{4}$$

ω_z, ω_c', ω_m are the axial, reduced cyclotron and magnetron frequency, respectively. One way to obtain the required free-ion cyclotron frequency ω_c from measurements of the three eigenfrequencies is to use the so-called invariance theorem [3]

$$\omega_\mathrm{c}^2 = \omega_\mathrm{c}'^2 + \omega_z^2 + \omega_\mathrm{m}^2 \tag{5}$$

which is independent of trap misalignments to first order. The sideband

$$\omega_\mathrm{c} = \omega_\mathrm{c}' + \omega_\mathrm{m} \tag{6}$$

can also be measured directly by excitation using a proper field geometry for the excitation.

Existing Penning trap mass spectrometers use different ways to detect the eigenfrequencies of the ions motion in the trap. At the University of Washington, Seattle [4], and at MIT, Boston [5], sensitive methods have been developed to detect the image currents induced in the trap electrodes by the ions oscillation. This allows non-destructive detection of the ionic resonances. A single ion can be kept in the trap virtually for ever and cooled to the ambient temperature which can be held at the boiling point of liquid He. In contrast Penning trap mass spectrometers at ISOLDE/CERN [6] and Stockholm [7] use a time of flight method developed by Gräff *et al.* [8] to detect excited ionic resonances in a destructive way. The ions are kicked out of the trap and their time of flight to a distant detector is measured. Since the ions spent only a short time in the trap, this method does not allow ion cooling to very low temperatures by resistive cooling except for highly charged ions and very high quality factors of the cooling circuit. For singly charged ions moderate cooling by buffer gas collisions may be employed [6]. It is, however, easy to inject ions from outside sources into the

[a] e-mail: `werth@mail.uni-mainz.de`
or e-mail: `werth@dipmza.physik.uni-mainz.de`

trap which is of advantage for the investigation of unstable isotopes or highly charged ions.

The accuracy of Penning trap mass spectrometer is basically limited by the stability and homogeneity of the magnetic field and the coherence time for the interaction of the trapped ion with the r.f. field which excites the motional oscillations. Statistical uncertainties of resonance frequencies below the ppb level are almost routinely obtained. In order to obtain the corresponding precision a careful account of possible systematic shifts of the eigenfrequencies is required. They stem mainly from trap imperfections, fluctuations of the magnetic field, and finite ion energies.

In this contribution we describe measurements in a Penning trap mass spectrometer which was used previously to determine the mass ratios of some light ions [9,10]. The present experiments deal with mass ratios of hydrogen and deuterium molecular ions to $^4He^+$ ions. Using the accepted values of the proton and deuteron mass we can calculated the atomic mass of ^{4}He. This may be of interest in view of some discrepancies between the accepted value [11] and a recently obtained value by the Stockholm group [12]. Preliminary values of our experiment have been published elsewhere [13].

2 Experiment

2.1 Experimental setup

Our experimental setup is described in some detail in reference [9]. We use a trap of characteristic dimension $d = 7.3$ mm, $\rho_0/z_0 = 1.16$, where ρ_0 is the trap radius, $2z_0$ the closest distance between the endcaps and $d = [\rho_0^2/2 + z_0^2]^{1/2}$. The electrodes are made from a copper-nickel alloy and carefully machined into hyperbolic shape to create a quadrupole potential. Adding ferromagnetic Ni to copper reduces the total susceptibility which is close to 0 at 3.99% part of Ni [14]. We have measured the susceptibility of our sample to -0.022×10^{-2} emu/g, which is a factor of 9.2 lower than oxygen-free copper which is usually employed in such devices. The electrodes were gold plated to reduce the chance of surface charges. The trap size has been chosen after extensive investigations on smaller and larger traps as a compromise between a small trapping volume and low distortion of the electrode shape. The endcap electrodes have central holes of 0.8 mm diameter for injection of electrons into the trap and for ejection of ions. Additional guard electrodes placed between the ring and endcaps as well as outside the endcaps near the entrance and exit holes serve to compensate for field imperfections caused by the truncation of the electrodes, possible misalignments or machining errors. The ring electrode is segmented into 4 equal quadrants to allow the application of radio-frequency fields in different coordinates. For isolation between the different electrodes we used Macor. The structure is made as symmetric as possible and uses a small amount of material to minimise the influence of the traps magnetic susceptibility on the magnetic field inhomogeneity. Figure 1 shows details of our trap.

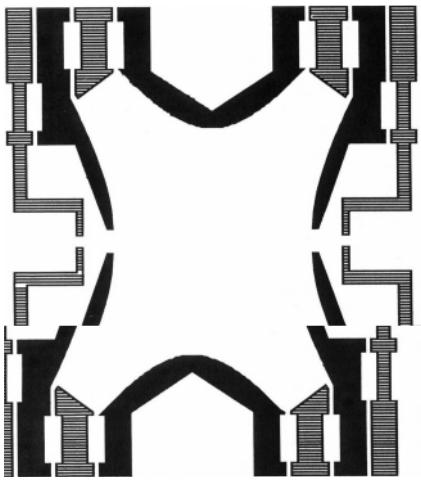

Fig. 1. Scale drawing of our trap structure. Full: main trap electrodes, hatched: correction electrodes. The axis of symmetry (z-axis) is in the horizontal direction. The closest distance between the endcap electrodes is 8.0 mm.

The trap was placed in the centre of a superconducting solenoid of 7 T field strength whose measured inhomogeneity was less than 1 part in 10^7 in a sphere of 5 mm diameter. The influence of external magnetic fields on the field strength at the ions position was reduced by a compensating coil [15]. The reduction factor was 30 as measured by application of a well defined dipole field outside the solenoid. Apart from short time intervals when the magnets cryostat was filled with liquid He or N_2 we did not observe a long term drift of the magnetic field at the 10^{-9} level.

The base pressure in our apparatus was 1×10^{-10} mbar as measured by an ionisation gauge at about half a meter distance from the trap. We used ionisation by electrons of the H_2 component of the background gas to create H_2^+ ions, while for experiments on He^+ or D_2^+ we introduced a small amount of He or D_2 through a needle valve. The measured pressure then was raised to about 3×10^{-10} mbar. At this pressure the collision limited coherence time of the ion in the trap was longer than 2 seconds.

2.2 Experimental procedure

After creation of ions inside the trap by an electron pulse of typically 10 ms length the ions are stored for 1 second and are then ejected from the trap. They were detected by a channel-plate multiplier placed at the end of our cryostat at about 50 cm distance from the trap (Fig. 2).

The magnetic field at the detector position was reduced to 0.25 T. Ions of different mass, created by the electron pulse, arrive at the detector at different times as seen in Figure 3 (left). A radio-frequency field applied between the traps endcap electrodes eliminates all ions from the trap whose axial frequency is resonantly excited by the field. We swept the frequency across a range which covered the axial oscillation frequency of all detected ion

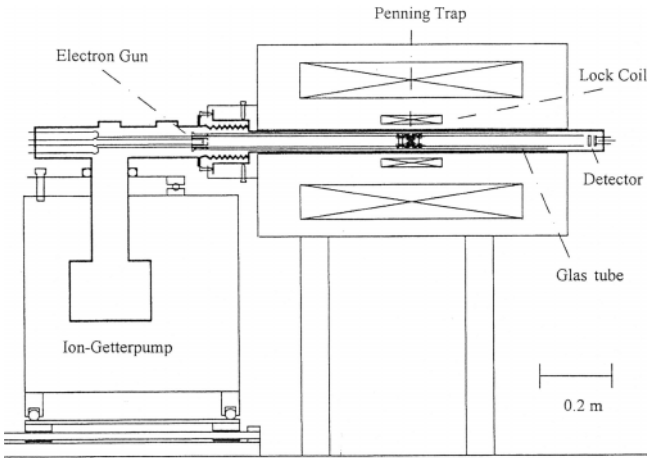

Fig. 2. Set-up of the experiment.

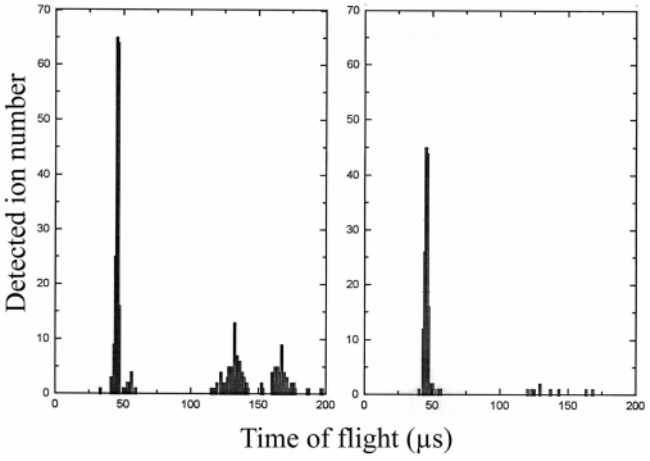

Fig. 3. Time-of-flight spectrum of ions created from the background gas by electroionisation. (Left): complete spectrum. The strong signal corresponds to mass 2 ions, the smaller ones to N_2^+, and O_2^+. (Right): remaining $m = 2$ ions after excitation of the axial resonance frequency of unwanted species.

species except that under investigation. Figure 3 (right) shows the result of such a cleaning procedure, which assures that in general no unwanted ion is left in the trap. We then reduced the electron current to such an amount that typically only in one out of three creation-detection cycles a single ion is detected. At a detection efficiency of our channel-plate of 30% this makes it sufficiently unlikely that more than a single ion is in the trap at the same time.

Cyclotron excitation is performed by an r.f. field applied between opposite parts of the segmented ring electrode. The effect of resonant excitation is to increase the radial energy. After ejection of the ions by a short electric pulse the increase in radial energy if transformed into axial energy by the fringe field of the magnet. This increase in axial energy reduces the flight time to the detector. We measure the average flight time to the detector which shows a minimum at resonant excitation.

The excitation starts after the cleaning period and lasts one second. The amplitude of the exciting r.f. field is set to a value which reduces the time-of flight to the

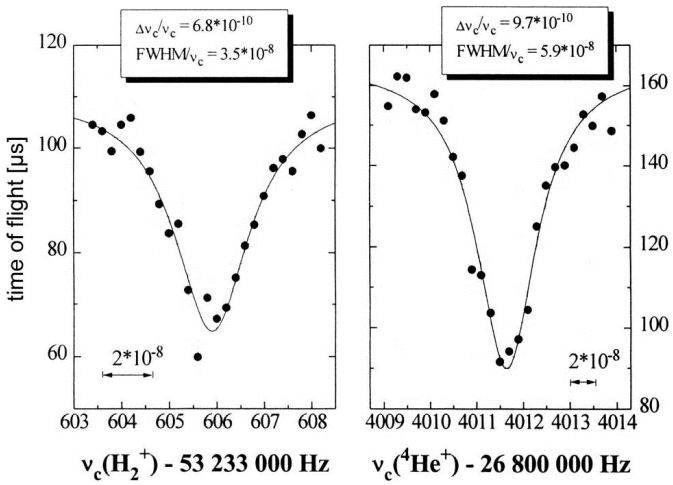

Fig. 4. Mean time-of flight for H_2^+ ions (left) and $^4He^+$ ions (right) when an azimuthal radio Frequency field is scanned around ω_c'. The full width corresponds to the Fourier limit of the excitation time of 1 s. The experimental data points are fitted by a Lorentzian line and the statistical uncertainty is below 1 ppb.

detector by typically 30%. A complete measurement of a cyclotron resonance consists of about 20 creation – detection cycles, during which the excitation frequency of several tens of MHz is varied in steps of 50 mHz around the resonance. To improve the signal-to-noise ratio each measurement was repeated 50 times. Test experiments with many more repetitions and a good signal-to-noise ratio demonstrated that the expected line shape and width is experimentally obtained. The line shape is given by the Fourier transform of the excitation period of length τ,

$$I(\omega - \omega_0) = I_0 \frac{\sin^2(\omega - \omega_0)\tau}{(\omega - \omega_0)^2} \tag{7}$$

where ω_0 is the resonance frequency and I_0 a normalising factor. Test measurements with extended averaging revealed the expected sidebands from equation (7). In our actual runs for mass comparison of two ions we did less averaging to reduce the total time of a measurement. The sideband structure was less visible and we used for simplicity a Lorentzian line shape to determine the centre frequency. Test of fits using the true and the simplified line shape showed that neither the centre frequency nor its uncertainty changed beyond the statistical expectations. The half width of the resonance, given by

$$\delta\omega_{1/2} = 0.89\tau^{-1} \tag{8}$$

agree well with the expectation. Figure 4 shows examples of the perturbed cyclotron frequencies for H_2^+ and $^4He^+$.

3 Systematic frequency shifts

While the statistical uncertainty in frequency of a cyclotron resonance line in general was well below the 1 ppb

level (see Fig. 4) the precision of a mass comparison is limited by the level at which systematic frequency shifts can be accounted for. Such frequency shifts arise from imperfections in the trap structure, machining errors, misalignments, or space charge, when several ions are confined simultaneously.

The influence of trap imperfections on the position of the motional resonances of a trapped ion has been calculated in detail by several authors [1,6,9,16]. The real potential of the trap can be expressed as a series expansion in terms of spherical harmonics:

$$V' = V_0 \Sigma C_k (\rho/d)^k P_k(\cos\theta) \tag{9}$$

V_2 is the ideal quadrupole potential

$$V_2 = \frac{V_0}{2d^2}\left(z^2 - \frac{\rho^2}{2}\right) \tag{10}$$

P_k are the spherical harmonics of order k and C_k denotes the strength of the perturbing potential of order k.

In a similar way the magnetic field can be expanded along the z-axis as

$$B = B_0 \Sigma b_k z^k. \tag{11}$$

The deviations of the electric and magnetic fields from the ideal form shift the cyclotron frequency by an amount which has been calculated in [1,6,9,16] up to the 4th order. If we include the next orders and assume spherical trap symmetry around the z-axis and reflection symmetry about the radial plane, for which the odd orders in the expansion vanish, we obtain the shift in frequency due to electrical imperfections [17]

$$\begin{aligned}\Delta\omega_c &= \Delta\omega_c' + \Delta\omega_m \\ &= \frac{\omega_z^2}{\omega_c'^2 - \omega_m}\left[\frac{3C_4}{4d^2}(\rho_m^2 - \rho_c'^2) + \frac{15C_6}{8d^4}\left(3z^2(\rho_m^2 - \rho_c'^2)\right.\right. \\ &\quad \left. + (\rho_c'^4 - \rho_m^4)\right) + \frac{35C_8}{16d^6}\left(18z^4(\rho_m^2 - \rho_c'^2)\right. \\ &\quad -24z^2(\rho_m^4 - \rho_c'^4) + 3(\rho_m^6 - \rho_c'^6) \\ &\quad \left.\left. + 6(\rho_m^4\rho_c'^2 - \rho_c'^4\rho_m^2)\right)\right]. \end{aligned} \tag{12}$$

Similarly for the magnetic case, the shift in frequency is given by

$$\begin{aligned}\Delta\omega_c &= \omega_c\frac{b_2}{2}\left(z^2 + \frac{\omega_m\rho_c'^2 - \omega_c'\rho_m^2}{\omega_c'' - \omega_m}\right) \\ &\quad + \omega_c\frac{b_4}{8}\left(3z^4 - 2\rho_m^2\rho_c'^2 + 12z^2\frac{\omega_m\rho_c'^2 - \omega_c'^2\rho_m^2}{\omega_c' - \omega_m}\right. \\ &\quad \left. -5\frac{\omega_c'\rho_c'^4 + \omega_m\rho_m^4}{\omega_c' - \omega_m} + \frac{\omega_c'\rho_m^4 - \omega_m\rho_c'^4}{\omega_c' - \omega_m}\right). \end{aligned} \tag{13}$$

Here z, ρ_c', ρ_m are the axial oscillation amplitudes and the radii of the reduced cyclotron and magnetron motion, respectively. In our experiment the largest contribution comes from the terms containing z. z can be as large as several mm, since it is given by the position of the ions at the instant of creation by electroionisation. This can be anywhere along the z-axis. The second largest part comes from terms containing ρ_m which can assume a maximal value of 0.4 mm, given by the radius of the electron entrance hole in the endcap compensation electrode. The radius of the reduced cyclotron orbit at our magnetic field strength of 7 T and a radial ion energy, which increases from 1/40 eV at creation to about 0.65 eV at resonant excitation is only 10 μm and terms containing higher orders in this coordinate can generally be neglected.

Finally an angle ε between the traps symmetry axis and the magnetic field direction shifts the cyclotron frequency by an amount [1,9]

$$\Delta\omega_c = \frac{9}{4}\omega_m \sin^2\varepsilon. \tag{14}$$

The maximal size of this angle in our experiment can be calculated from the size of the entrance and exit holes in the endcap compensation electrodes of 0.8 mm diameter, considering the fact that the electron beam to create ions starts from a source outside the trap, travels along a magnetic field line and passes through both the holes. We obtain $\varepsilon_{max} = 0.2°$.

As shown by Brown and Gabrielse [1], equation (5) is independent of a tilt angle ε to first order. A measurement of all three frequencies thus would virtually eliminate this uncertainty in the determination of ω_c. In our experiment, however, we cannot measure the axial frequency ω_z sufficiently accurate and thus cannot make use of this property.

3.1 Minimising frequency shifts

From equations (12, 13) it is obvious that there are two ways to minimise shifts of the cyclotron frequency imposed by trap imperfections: reduction of higher order contributions to the trapping potential and the magnetic field as well as reduction of the ion oscillation amplitudes. Both ways have been pursued in our experiment.

3.1.1 Reduction of the axial oscillation amplitude

Initially the ions are created at a low trapping voltage (150 mV). After creation the voltage is raised to 1850 mV. If the voltage increase is performed adiabatically ($Vt^{-1}/\omega_z V \ll 1$) the amplitude decreases by the 4th root of the ratio of the final to initial voltage [9], in our case by nearly a factor 2. If we assume reasonably that the ion creation is distributed with equal probability along the z-axis, the initial mean axial oscillation amplitude of 2.1 mm is reduced to about 1 mm. This is still larger than the cyclotron and magnetron radius and thus gives rise to the largest contribution to frequency shifts according to equations (12, 13).

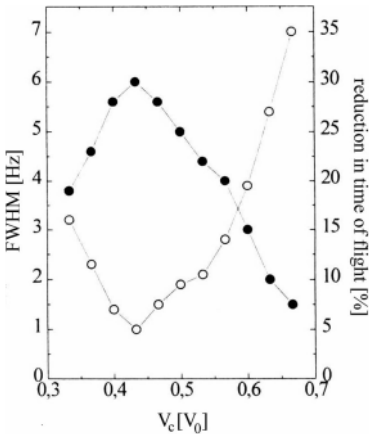

Fig. 5. Full width of the cyclotron frequency of H_2^+ ions (open circles) and reduction in time-of-flight to the detector at resonant excitation (full circles) for different voltages V_c applied to the correction electrodes between ring and endcaps. The voltages are given in units of the trap voltage V_0. For $V_c = 0.43V_0$ the minimum in linewidth and the maximal change in time-of-flight indicate the optimum correction voltage to minimise higher order contributions to the trapping potential.

3.1.2 Tuning the trap

Voltages V_c applied to the guard electrodes between ring and endcap as well as outside the endcap electrodes serve to minimise higher order contributions to the trapping potential. We calculated the necessary voltages to minimise simultaneously the coefficients C_4 and C_6 in the series expansion of the potential (Eq. (9)) using the program SIMION [18]. Without any applied correction voltage the coefficients C_4 and C_6 are calculated as 0.13 and 3.1, respectively. Simultaneous minimisation appeared in the simulation at correction voltages of $V_c = 0.461V_0$ for the radial correction electrodes and $V_h = 2.259V_0$ for the endcap correction electrodes. At these voltages the coefficients C_4 and C_6 assume a value of 2×10^{-5} and -6×10^{-4}, respectively. When we tuned these voltages experimentally, we found that the linewidth of the reduced cyclotron resonance shows a distinct minimum at a certain value of the correction voltage V_c. At the same voltage the change in time-of-flight of the ions to the detector after resonant excitation shows a maximum (Fig. 5). We obtained experimentally a value of $V_c = 0.43V_0$, which agrees reasonably well with the calculated value. Also the lineshape of the resonance becomes asymmetric for wrong values of the correction voltage and symmetric for a well tuned trap (Fig. 6). No significant change on the resonance line was found upon variation of V_h and we used the calculated value for our measurements. We estimate the uncertainty in the calculated values of the correction voltages to 10^{-2}. We use this uncertainty later on to estimate the remaining frequency shifts arising from trap imperfections.

3.1.3 Magnetic field inhomogeneities

The magnetic field along the z-axis was measured by the frequency of the ions cyclotron resonance when the trap was moved along the field direction. The obtained data points could be well fitted by a parabola and we obtained a coefficient $b_2 = 4.3 \times 10^{-9}$ mm^{-2} for a quadratic contribution to the magnetic field. The value of the quadratic field distortion by the traps susceptibility was calculated to 9×10^{-10} mm^{-2}.

3.1.4 Ion-ion interaction

The Coulomb potential of different simultaneously confined ions in the trap represents a perturbation of the trapping potential and thus may cause a shift of the eigenfrequencies. Although we kept the number of detected ions in each measuring cycle low, there is a chance to have several ions at the same time in the trap due to the statistical nature of the ion creation in the trap and the detection process of the channel plate. Assuming a Poisson distribution for the detection probability we have for an average detected ion number of $n = 0.3$, as typical for our experiment, chances of 74%, 22% and 3% to detect 0, 1 or 2 ions, respectively, in each cycle.

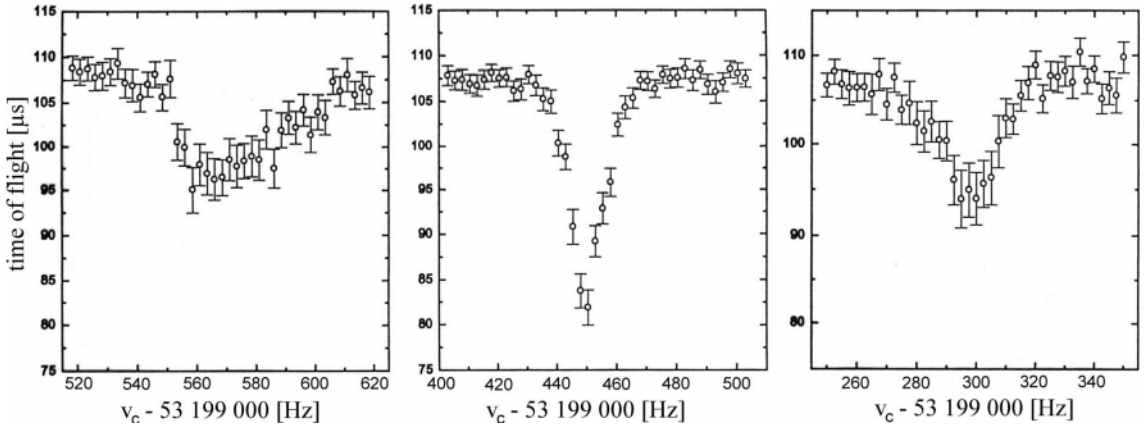

Fig. 6. Cyclotron resonances ω_c' for different correction voltages: $V_c = 0.3$, 0.43, and $0.65V_0$ (from left to right) indicating line asymmetries for distorted trap potentials.

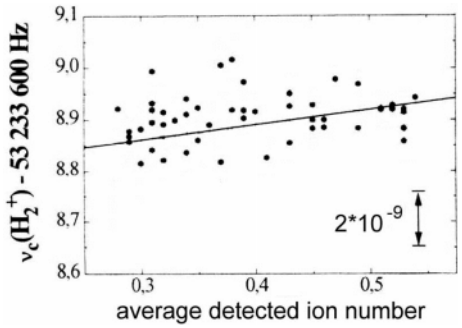

Fig. 7. Shift of the cyclotron frequency at different detected H_2^+ ion numbers n. A linear fit through the experimental values gives a dependence $\delta\omega_c = 0.29(6)n$ [Hz].

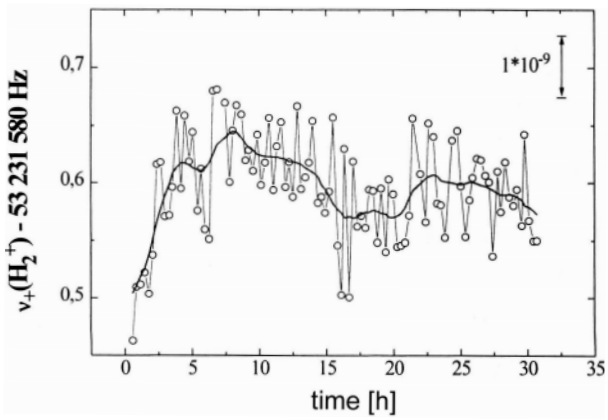

Fig. 8. Temporal stability of the magnetic field from our superconducting solenoid. Data were taken every 20 min. The solid line is the average of 7 adjacent data points.

We have measured the shift of the cyclotron frequencies for different detected ion numbers n. Figure 7 shows an example for H_2^+. From a linear fit to the data we obtain shifts of 0.29 (6) Hz/n for H_2^+, 0.175 (21) Hz/n for D_2^+, and 0.15 (3) Hz/n for $^4He^+$.

3.1.5 Temporal magnetic field instabilities

Precise mass measurements require that the cyclotron frequencies of different ions are compared at the same magnetic field. As it is well known, the field of superconducting solenoids may exhibit temporal drifts and jumps, caused by pressure changes in the magnets cryostat, by flux quantum jumps or by varying ambient fields. We have measured the temporal variation of our magnetic field by monitoring the cyclotron frequency of an ion over an extended period of time. Figure 8 shows a typical example. We took data points every 20 min over a period of 30 hours. The magnetic field shows variations of the order of 10^{-9}. They appear in a random manner and no systematic drift is seen. To reduce the possible influence of short term variations on the position of the cyclotron resonances of different ions we changed between two ion species after each

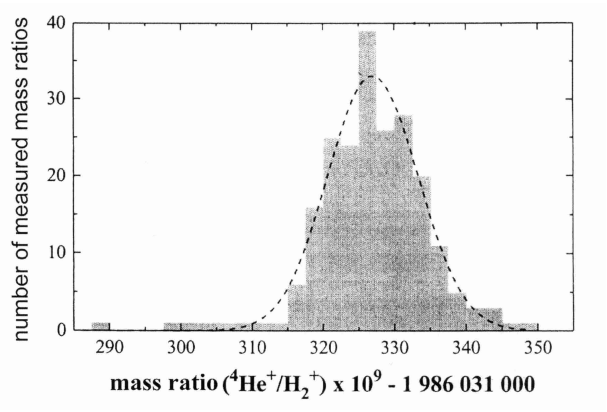

Fig. 9. Histogram of 216 values of $^4He^+/H_2^+$ mass ratios, derived from their cyclotron resonances. The shape is nearly a Gaussian (dotted line). The uncertainty of the mean is 1.5×10^{-10}.

data point when we scanned the applied radio frequency. The change was effected every 1.3 minutes. Checks on the statistical distribution of the measured frequency ratios did not show any deviation from the expectation beyond statistical scatter. So we conclude that time variation of the magnetic field does not contribute to the error significantly at our level of precision.

4 Measurements

After setting the voltages of the correction electrodes to the optimum values we excited the sideband resonance at $\omega_c = \omega_c' + \omega_m$ by a radio-frequency field applied between two adjacent quadrants of the ring electrode. Comparison of two different ions took place, as mentioned above, by switching between the different ions after each frequency point. The average time-of-flight for each data point was determined after 50–100 measuring cycles. The data points for each ion were fitted by a Lorentzian line shape. The statistical uncertainty of the line centre generally was below 1 ppb as seen in Figure 4. The measurements were repeated many times. A histogram of the frequency ratio for two different ions shows a Gaussian distribution (Fig. 9), from which the mean was taken. Data were taken for $^4He^+/H_2^+$ and $^4He^+/D_2^+$ mass ratios.

An additional measurement on the $^4He^+/D_2^+$ mass ratio was performed by an excitation of the frequency $2\omega_c'$. This resonance could be observed at higher excitation amplitudes. The magnetron frequency, required for the calculation of ω_c, was determined from the difference of ω_c' and ω_c. The magnetron frequency shows only a small dependence on the mass of the ions and its values were determined as 376.69 (24) Hz and 376.17 (35) Hz for D_2^+ and $^4He^+$, respectively. Statistical checks were made in a similar way as described above and no deviation from a purely statistical scatter of the data was found.

Table 1. Fractional uncertainties from trapping field imperfections, ion-ion interaction and relativistic mass shifts on the mass ratios of $^4He^+/H_2^+$ and $^4He^+/D_2^+$.

Source of error	$^4He^+/H_2^+$	$^4He^+/D_2^+$
$C_4(2\times10^{-5})$	7.8×10^{-11}	4.7×10^{-13}
$C_6(-6\times10^{-4})$	4.5×10^{-11}	2.7×10^{-13}
$b_2(4.3\times10^{-9}\ \mathrm{mm}^2)$	2.5×10^{-11}	1.1×10^{-11}
$\varepsilon_{\max}(0.2^0)$	4.1×10^{-10}	2.5×10^{-12}
ion–ion	1.9×10^{-9}	1.3×10^{-10}
rel. mass shift	3.2×10^{-10}	2.5×10^{-13}
quadratic sum	2.0×10^{-9}	1.4×10^{-10}

5 Systematic errors

The frequency shifts arising from the residual values of the higher order contributions in the trapping potential as discussed in Section 3.1.2 as well as from the second order coefficient b_2 in the magnetic field from Section 3.1.3 were calculated. Their influence on the mass ratios are listed in Table 1. They are in all cases below 10^{-10} and can be neglected compared to the statistical uncertainty. The uncertainty from a possible angle $\varepsilon_{\max}$ between the trap axis and the magnetic field direction (Eq. (14)) is negligible for the mass doublet $^4He^+/D_2^+$, since it cancels out in the first order, but contributes to the error budget for non-doublets. Similarly the effect of ion-ion interaction can be neglected for doublets, but represents in our case the largest systematic uncertainty for the mass ratios for a non-doublet.

Finally a shift of the cyclotron frequencies arises from the second order Doppler effect. The ions energy is increased by the excitation process from initially thermal values. From the measured shape of the magnetic field strength along the axis between the trap and the detector and the measured reduction in flight time at resonant cyclotron excitation we calculate that the maximum energy of the detected ion was 0.65 eV. We take this value to calculate the maximum relativistic shift and its influence on the mass ratio.

From the quadratic sum of the systematic uncertainties in Table 1 we find that in case of the mass doublet $^4He^+/D_2^+$ the systematic error is smaller than the statistical uncertainty while for the non-doublet $^4He^+/H_2^+$ the systematic uncertainty dominates.

6 Results and discussions

The results of our mass comparisons for $^4He^+/H_2^+$ and $^4He^+/D_2^+$ are

$$^4He^+/H_2^+: \quad 1.986\,031\,327\,4\,(31) \qquad (1.5\times10^{-9}),$$
$$^4He^+/D_2^+: \quad 0.993\,643\,871\,28\,(55) \qquad (0.6\times10^{-9}).$$

The quoted uncertainties are the quadratic sum of the statistical and systematical uncertainties. For the $^4He^+/D_2^+$ case we have combined our results from the independent determinations by ω_c and $2\omega_c'$ which gave the same numbers within the statistical error.

Table 2. Mass values for atomic ^{4}He.

4.002 603 248 9 (22)	this work
4.002 603 256 8 (13)	reference [12]
4.002 603 249 7 (10)	accepted value [19]

From the mass ratios we can calculate the mass values for the neutral helium atom. When we use the accepted values for the proton and deuteron mass from the most recent CODATA compilation [19] and the known values for the ionisation and dissociation energies of the atoms and molecules (including a small correction for the average vibrational quantum number of the molecules $\hat{\nu} = 3.5$ [20,21]) we obtain for $m(H_2^+) = 2.015\,101\,497\,03\,(36)$ au and $m(D_2^+) = 4.027\,654\,988\,04\,(70)$ au. It the follows for the mass of the neutral ^{4}He atom:

from $^4He^+/H_2^+$:
$m(^4\mathrm{He}) = 4.002\,603\,254\,5\,(63)$ au $\qquad (1.5\times10^{-9})$,

from $^4He^+/D_2^+$:
$m(^4\mathrm{He}) = 4.002\,603\,248\,2\,(24)$ au $\qquad (0.6\times10^{-9})$.

In Table 2 we list the weighted mean of these results along with other recently obtained values.

Our final result is in agreement to the accepted value of the ^{4}He mass. It deviates from the recently obtained value by the SMILTRAP group. It has been suggested [12] that this discrepancy might be due to a proton mass different from the accepted value as is was indicated by earlier measurements of the SMILETRAP group [22]. Although our error bar is somewhat larger than those by previous experiments our result may help to obtain a reliable and accurate mass value. Results at the 1 ppb level of precision "should not remain unchallenged: checks by another group, at the same level of precision, are highly desirable to strengthen the validity of their mass measurements, and transform these very precise measurements into very accurate ones" [G. Audi]. Further improvement of our result would theoretically be possible when the largest uncertainty in our experiment arising from the ion-ion interaction would be reduced. This requires a further reduction of the average detected ion number n. Since this is already as low as $n = 0.3$ or even below it would increase the total time for a measurement unless the detection efficiency can be enhanced significantly. This has the risk of temporal instabilities of the magnetic field and also of the electric trapping field. Thus we conclude that further improvements of our present technique is limited by practical constraints.

Our experiments were supported by the Deutsche Forschungsgemeinschaft. We thank R. Ley for careful checking our calculations and A. Drakoudis for help with the manuscript.

References

1. L. Brown, G. Gabrielse, Rev. Mod. Phys. **58**, 233 (1986).
2. F. Vedel, G. Werth, in *Practical Aspects of Ion Trap Mass Spectrometry*, edited by R.E. March, J.F. Todd (CRC Press, Boca Raton, 1995), Vol. II, p. 237.
3. L.S. Brown, G. Gabrielse, Phys. Rev. A **25**, 2423 (1982).
4. F.L. Moore, D.L. Farnham, P.B. Schwinberg, R.S. van Dyck Jr, Nucl. Instr. Meth. B **43**, 425 (1989).
5. E.A. Cornell *et al.*, Phys. Rev. Lett. **63**, 1674 (1989).
6. G. Bollen, R.B. Moore, G. Savard, H. Stolzenberg, J. Appl. Phys. **68**, 4355 (1990).
7. R. Jertz *et al.*, Z. Phys. D **21** , 179 (1991).
8. G. Gräff, H. Kalinowsky, J. Traut, Z. Phys. A **297**, 35 (1980).
9. Ch. Gerz, D. Wilsdorf, G. Werth, Nucl. Instr. Meth. B **47**, 453 (1990).
10. D. Hagena, G. Werth, Europhys. Lett. **15**, 491 (1991).
11. R.S. van Dyck Jr *et al.*, in *Trapped Charged Particles and Fundamental Physics*, edited by D. Dubin, D. Schneider (AIP Conf. Proc. No 457, 1999), p. 101.
12. T. Fritioff *et al.*, Eur. Phys. J. D (accepted).
13. S. Brunner *et al.*, in *Trapped Charged Particles and Fundamental Physics*, edited by D. Dubin, D. Schneider (AIP Conf. Proc. No 457, 1999), p. 125.
14. E.W. Pugh, F.M. Ryan, Phys. Rev. **111**, 1038 (1958).
15. G. Gabrielse, J. Tan, J. Appl. Phys. **63**, 5143 (1988).
16. M. Kretzschmar, Z. Naturf. **45a**, 965 (1990).
17. H. Klein, Diplomarbeit, Mainz, 1996.
18. SIMION 3D, Version 6.0, Idaho Natl. Eng. Lab. (1995).
19. P.J. Mohr, B.N. Taylor, J. Phys. Chem. Ref. Data **28**, 1713 (1999).
20. F. von Busch, G. Dunn, Phys. Rev A **5**, 1726 (1972).
21. Y. Weijun, R. Alheit, G. Werth, Z. Phys. D **28**, 87 (1993).
22. C. Carlberg, Hyperf. Interact. **114**, 177 (1998).